

Certified quantum gates

Wesley C. Campbell

University of California Los Angeles, Los Angeles, California 90095, USA



(Received 30 March 2020; accepted 10 August 2020; published 31 August 2020)

High quality, fully programmable quantum processors are available with small numbers (< 1000) of qubits, and the scientific potential of these near-term machines is not well understood. If the small number of physical qubits precludes practical quantum error correction, how can these error-susceptible processors be used to perform useful tasks? We present a strategy for developing quantum error detection for certain gate imperfections that utilizes additional internal states and does not require additional physical qubits. Examples for adding error detection are provided for a universal gate set in the trapped-ion platform. Error detection can be used to certify individual gate operations against certain errors, and the irreversible nature of the detection allows a result of a complex computation to be checked at the end for error flags.

DOI: [10.1103/PhysRevA.102.022426](https://doi.org/10.1103/PhysRevA.102.022426)

For the near-term future, it is likely that the quantum information processors that become available will be capable of running intermediate-scale algorithms in the presence of multiple (possibly numerous) errors [1]. For beyond-classical computations in this paradigm, the result reported by the quantum computer is almost guaranteed to be wrong, and the recent observation of quantum advantage by the Google group [2] was made possible only by arguing that, after repeating the algorithm many times, the algorithmic error probability could be made statistically distinguishable from 1. For algorithms where the result can be tested directly for correctness (such as Shor's factoring algorithm [3]), this may be useful, at least up to the point where the ratio of the runtime-to-success probability exceeds practical timescales. However, for many applications of quantum computers (such as the sampling problem used to demonstrate quantum advantage, and much of quantum simulation), the user has very little idea which results are the trustworthy ones, potentially rendering any purported quantum advantage effectively useless. Quantum advantage is likely necessary, but not generally sufficient, to realize quantum utility beyond classical machines.

Here, following recent work that demonstrated a related technique to herald and suppress asymmetric leakage of population from the qubit subspace [4], we consider the issue of how to deal with errors in quantum processors caused by imperfections in the applied gates. While the techniques we outline below are applicable to other hardware platforms, we present them in the context of trapped-ion hyperfine qubits, which are effectively free of errors outside of those caused by the gates themselves. In particular, since frequency stability is typically easier to distribute, assess, and achieve than amplitude stability, errors caused by frequency drifts are usually unlikely compared with errors in the areas of pulses applied to perform gates, and we therefore focus primarily on amplitude errors. Composite pulse sequences [5] can be used to suppress amplitude (and frequency) errors that are common mode for the duration of a composite pulse sequence but do not perform

well against correlated errors that are not constant during the sequence, such as amplitude drifts from amplifier temperature changes or laser intensity noise. Far from being exotic or implausibly insidious, these types of amplitude-drift errors, which degrade the protection afforded by composite pulse sequences, have posed obstacles for a number of experiments working at the forefront of fidelity [6–8].

In this paper, we present a strategy for designing certifiable gates that uses auxiliary states in each qubit host and does not require additional physical qubits. The larger Hilbert space afforded by including ancillary states allows us to restructure a gate as a series of population-transfer steps that are each followed by dissipation of the error state through coupling to a bath or detector. Specifically, each step is designed as a rotation from the initial state $|\psi_n\rangle$ to an orthogonal target state $|\psi_{n+1}\rangle$. By choosing $|\psi_n\rangle$ and $|\psi_{n+1}\rangle$ to reside in orthogonal Hilbert spaces, this rotation can be attempted and certified without acquiring knowledge of the information encoded in either state. If the execution of this rotation is imperfect due to an error in the degree of the rotation (i.e., the amplitude), the system will be left in $|\phi_{n+1}\rangle \approx |\psi_{n+1}\rangle + \epsilon|\psi_n\rangle$, and subsequent detection that the system is not in the error state $|\psi_n\rangle$ certifies the step against the rotation error. Since the dissipative detection step is irreversible, testing for errors can be done either during the computation or at the end, and checking a result for error flags can serve as a limited test of the trustworthiness of the result.

We begin with an example that illustrates the main idea in the form of arbitrary single-qubit gates that the user can certify against single-pulse amplitude errors. Examples of how to certify against errors in multiqubit contexts such as addressing errors and two-qubit entangling gate errors are also presented, demonstrating that a complete set of gates for universal quantum computing can be augmented with certification against some classes of errors.

We consider a system consisting of a qubit ($|0\rangle$ and $|1\rangle$) and two additional long-lived auxiliary states $|A^{(+)}\rangle$ and $|A^{(-)}\rangle$ that

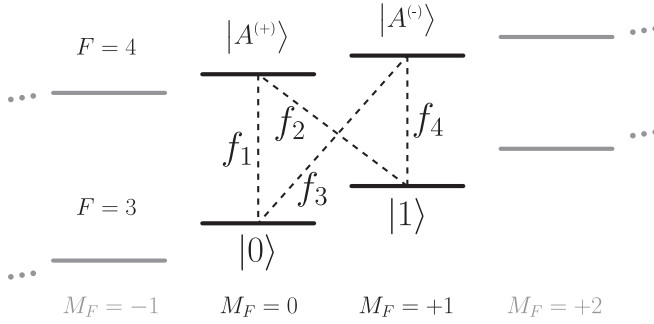


FIG. 1. Example $^2F_{7/2}$ state encoding of the qubit and auxiliary states in $^{171}\text{Yb}^+$. For storage, the qubit can be encoded in the two clock states and then transferred to and from this arrangement before and after gates. All four transitions are within Zeeman shifts of the zero-field hyperfine splitting of 3.602(2) GHz [9].

can each be coupled to both qubit states via resonant radiation. For concreteness, we suppose that the qubit and auxiliary states are encoded in Zeeman sublevels of the effectively stable $^2F_{7/2}^o$ state of $^{171}\text{Yb}^+$, shown in Fig. 1. The qubit states can be defined as $|0\rangle \equiv |F, M_F\rangle = |3, 0\rangle$ and $|1\rangle \equiv |3, 1\rangle$, and the auxiliary states as $|A^{(+)}\rangle \equiv |4, 0\rangle$ and $|A^{(-)}\rangle \equiv |4, 1\rangle$. A stable, static magnetic field provides the qubit splitting, and the qubit and auxiliary manifolds are separated by the $^2F_{7/2}^o$ hyperfine splitting (≈ 3.6 GHz; we refer to the coupling fields as microwaves). Furthermore, we require that the system possess a means by which projective quantum measurement can be performed selectively for population in each of these two manifolds. In this example, detection can be effected by hyperfine-selective transfer to the ground $^2S_{1/2}$ state via optical pumping at $\lambda = 760$ nm on $^1[3/2]_{3/2}^o \leftarrow ^2F_{7/2}^o$, followed by spontaneous emission on $^1[3/2]_{3/2}^o \sim ^2S_{1/2}$. We have confirmed experimentally that this measurement can be accomplished in a few milliseconds with greater than 95% hyperfine manifold selectivity [10], and the theoretical limit is greater than $1 - 10^{-5}$.

Without loss of generality, we adopt a state vector description of the gate operation for clarity. Before we describe the certified gate protocol, we can consider the action of a general, unitary, single-qubit gate $U(\hat{\mathbf{n}}, \Theta) \equiv \exp(-i\Theta \hat{\mathbf{n}} \cdot \boldsymbol{\sigma}/2)$ on an arbitrary pure input state $|\psi_0\rangle \equiv \alpha|0\rangle + \beta|1\rangle$. If we rewrite the initial state in the basis of $|\pm n\rangle$ (the \pm eigenvectors of $\hat{\mathbf{n}} \cdot \boldsymbol{\sigma}$), we have

$$|\psi_0\rangle = c^{(+)}|+n\rangle + c^{(-)}|-n\rangle, \quad (1)$$

where $c^{(\pm)} \equiv \langle \pm n | \psi_0 \rangle$. The states $|\pm n\rangle$ can likewise be written in terms of the polar (θ) and azimuthal (ϕ) angles of $\hat{\mathbf{n}}$ on the Bloch sphere as

$$\begin{aligned} |+n\rangle &= \cos\left(\frac{\theta}{2}\right)|0\rangle + e^{i\phi}\sin\left(\frac{\theta}{2}\right)|1\rangle, \\ |-n\rangle &= \sin\left(\frac{\theta}{2}\right)|0\rangle - e^{i\phi}\cos\left(\frac{\theta}{2}\right)|1\rangle. \end{aligned} \quad (2)$$

This choice of basis simplifies the expression describing the effect of the gate to

$$U(\hat{\mathbf{n}}, \Theta)|\psi_0\rangle = e^{-i\frac{\Theta}{2}}c^{(+)}|+n\rangle + e^{i\frac{\Theta}{2}}c^{(-)}|-n\rangle. \quad (3)$$

For a certifiable version of the gate $U(\hat{\mathbf{n}}, \Theta)$, first, a microwave pulse with four simultaneous tones (f_i , see Fig. 1) transfers (ideally all) the population from the qubit states to the auxiliary states according to $|\pm n\rangle \rightarrow |A^{(\pm)}\rangle$. Each of the $|\pm n\rangle$ basis states is paired with only one of the auxiliary states $|A^{(\pm)}\rangle$ by two of the four tones f_i and acts as a coherent dark state with respect to the other two. The relative phases φ_{12} and φ_{34} and Rabi frequencies Ω_i chosen for the four frequencies depend only on the angles used to describe $\hat{\mathbf{n}}$, ϕ , and θ [respectively, see Eq. (2)]. Specifically, $\varphi_{12} = \varphi_{34} - \pi = \phi$, $\Omega_1 = \Omega_4 = \Omega \cos(\theta/2)$, and $\Omega_2 = \Omega_3 = \Omega \sin(\theta/2)$. In the rotating frame with respect to the four splittings, the interaction Hamiltonian is

$$H = |A^{(+)}\rangle \left(\frac{\Omega_1}{2}|0\rangle + \frac{\Omega_2}{2}e^{-i\phi}|1\rangle \right) + |A^{(-)}\rangle \left(\frac{\Omega_3}{2}|0\rangle + \frac{\Omega_4}{2}e^{-i(\phi+\pi)}|1\rangle \right) + \text{H.c.} \quad (4)$$

$$= \frac{\Omega}{2}(|A^{(+)}\rangle\langle+n| + |A^{(-)}\rangle\langle-n| + \text{H.c.}), \quad (5)$$

where we assume the splittings are such that the four frequencies are nondegenerate.

Since these four sinusoids can be generated by a single synthesizer (for instance, a digital arbitrary waveform generator utilizing a single voltage reference) and can be made to share a single transmission system, amplifier chain, antenna, etc., we consider the case in which the amplitude error of this step is a fractional amplitude error that is shared by all four coupling terms. Since we seek full transfer from the qubit manifold to the auxiliary manifold, we represent the pulse area as $\int dt \Omega = \pi + \delta\pi_n$, where $\delta\pi_n$ is the result of an amplitude error for the n th step of the gate. We can write the state of the system after the (possibly imperfect) transfer as

$$\begin{aligned} |\phi_1\rangle &= -i \cos\left(\frac{\delta\pi_1}{2}\right) (c^{(+)}|A^{(+)}\rangle + c^{(-)}|A^{(-)}\rangle) \\ &\quad - \sin\left(\frac{\delta\pi_1}{2}\right)|\psi_0\rangle, \end{aligned} \quad (6)$$

which is in the desired form for error detection,

$$|\phi_{n+1}\rangle = \sqrt{1 - |\epsilon|^2}|\psi_{n+1}\rangle + \epsilon|\psi_n\rangle, \quad (7)$$

if we identify the error as $\epsilon = -\sin(\delta\pi_1/2)$.

Next, any population left in the qubit manifold ($|0\rangle$ and $|1\rangle$, see Fig. 1) is dissipatively transferred to $^2S_{1/2}$ via optical pumping. This ‘‘clean out’’ process will be accompanied by subsequent fluorescence detection of ground-state population at some point—right away or potentially even up until the very end of an algorithm. If the ion is queried immediately, it will yield fluorescence (a ‘‘bright-state ion’’) with small probability $\sin^2(\delta\pi_1/2)$. If the ion is not in the bright state, the dissipative process has completed the successful transfer of all qubit population to the auxiliary manifold, yielding the desired target state free of that error, $|\psi_1\rangle = -i(c^{(+)}|A^{(+)}\rangle + c^{(-)}|A^{(-)}\rangle)$.

For the third step, a second pulse with the same four tones is applied to transfer (ideally all) the population from the auxiliary manifold back to the qubit manifold. The only difference between the waveform for the first and second

pulses is that a common phase shift $\pi - \Theta/2$ is added to tones f_1 and f_2 only, and a common phase shift of $\pi + \Theta/2$ is added to tones f_3 and f_4 only. Again keeping track of a potential (possibly different) amplitude error that gives rise to finite $\delta\pi_2$ in the nominal π pulse, the system is left in

$$|\phi_2\rangle = \cos\left(\frac{\delta\pi_2}{2}\right)(e^{-i\frac{\Theta}{2}}c^{(+)}|+n\rangle + e^{i\frac{\Theta}{2}}c^{(-)}|-n\rangle) - \sin\left(\frac{\delta\pi_2}{2}\right)|\psi_1\rangle, \quad (8)$$

which is in form (7) for $\epsilon = -\sin(\delta\pi_2/2)$.

As the final step, any population left in the auxiliary manifold ($|A^{(\pm)}\rangle$, viz. $|\psi_1\rangle$) is optically pumped to the ground state, either yielding a bright state (with probability $\sin^2(\delta\pi_2/2)$) or completing the transfer to produce

$$|\psi_2\rangle = U(\hat{\mathbf{n}}, \Theta)|\psi_0\rangle = e^{-i\frac{\Theta}{2}}c^{(+)}|+n\rangle + e^{i\frac{\Theta}{2}}c^{(-)}|-n\rangle, \quad (9)$$

the ideal gate with no contribution from the amplitude errors.

The gate protocol above provides a means for certifying the operation against fractional amplitude errors that are shared by the four tones in either of the two pulses. With respect to this error model, whether we check for a bright state immediately or delay the flag query, the dissipative transfer of leftover population to the bright state either leaves the ion in the bright state or accomplishes errorless operation of the gate. The overall probability of error-free operation is $[1 - \sin^2(\delta\pi_1/2)][1 - \sin^2(\delta\pi_2/2)] \approx 1 - 2(\delta\pi/2)^2$ (where $\delta\pi$ is an average error during this sequence) and for uncorrelated errors, the overall error probability is $\sqrt{2}$ larger than the case without the out-coupling for error detection [$\approx \sqrt{2}(\delta\pi/2)^2$]. For single, isolated gates, this accomplishes no error correction, but the error detection can be used as a means to select instances that are trustworthy against this type of error. For instance, the high-quality rotations that are required to perform quantum state or process tomography could be certified against conflating errors in the state or process with this type of error introduced by the tomography process. Perhaps more importantly, more trustworthy NISQ-era [1] computational results can be sorted from those that are flagged by this process as containing errors, which may prove a useful way to assess the confidence of a result.

The gate certification idea above is also extendable to multiqubit gates and other types of errors. Next, we consider two examples of particularly troublesome error sources in the trapped ion platform: qubit addressing errors, and errors in two-qubit entangling gates.

For trapped ions with hyperfine qubits, an addressed single-qubit gate can be driven by a focused laser beam where the “microwave” signals are actually in optical beat notes that drive stimulated Raman transitions. If the first step of the certified single-qubit gate described earlier is applied to ion j by one such laser beam, there can be a non-negligible amount of light that illuminates neighboring ions and moves a small amount of their qubit populations to their auxiliary manifolds. To deal with this, the optical pumping beam addressed to ion j can be augmented by a series of optical pumping beams on the neighboring ions (or further) that are tuned to clean out those ions’ auxiliary manifolds. This will either flag an addressing error by producing a bright state, or, more likely,

undo any errant transfer from imperfect addressing by the stimulated Raman beam. The same process can then be applied for the second half of the gate being run on ion j , except that now the clean out will have all optical pumping beams (including j) set to clean out the auxiliary manifolds. Addressing errors of the optical pumping beams themselves are still possible in the first half of the gate, but these will also be flagged by the appearance of a bright state. A lack of bright-state qubits, therefore, certifies the gate against both Raman beam and optical pumping beam addressing errors—if all ions are found to be dark, these addressing errors have been eliminated.

For multiqubit gates, we choose as an example the Cirac-Zoller (CZ) gate [11] since it maps easily onto a series of discrete population transfer steps. We consider two ions (m and n) in arbitrary initial qubit states and one motional mode of frequency ν prepared in its ground state. Frequency selectivity can be used to drive “carrier” ($\sigma_+ + \sigma_-$), “red sideband” ($a\sigma_+ + a^\dagger\sigma_-$), or “blue sideband” ($a^\dagger\sigma_+ + a\sigma_-$) transitions, where σ_\pm and a^\dagger , a are the atomic and motional raising and lowering operators, respectively. To be consistent with the original proposal by Cirac and Zoller and to avoid confusion with motional Fock state labels, we adopt $|e_{m/n}\rangle$ and $|g_{m/n}\rangle$ as the notation for the qubit states.

A certifiable version of the CZ gate proceeds in four transfers, shown in Fig. 2. We start with an initial (possibly entangled) state $|\psi_0\rangle = (c_{ee}|e_m, e_n\rangle + c_{ge}|g_m, e_n\rangle + c_{eg}|e_m, g_n\rangle + c_{gg}|g_m, g_n\rangle) \otimes |0\rangle$. First, two simultaneous tones (on a non-copropagating stimulated Raman beam) are applied to only ion m such that $f_1 + \nu$ transfers $|e_m, 0\rangle \rightarrow |A_m^{(+)}, 1\rangle$ (i.e., on a blue sideband) and f_4 drives $|g_m, 0\rangle \rightarrow |A_m^{(-)}, 0\rangle$ (carrier). This is followed by hyperfine-resolved optical pumping of any residual population in qubit manifold of ion m to $^2S_{1/2}$. If ion m is not found in the bright state after this process [the probability of which is $1 - \sin^2(\delta\pi_1/2)$], the system will be left in the state

$$|\psi_1\rangle = -i(c_{ee}|A_m^{(+)}, e_n, 1\rangle + c_{eg}|A_m^{(+)}, g_n, 1\rangle + c_{ge}|A_m^{(-)}, e_n, 0\rangle + c_{gg}|A_m^{(-)}, g_n, 0\rangle). \quad (10)$$

Second, three frequencies will be applied simultaneously and individually addressed as follows: Ion m will be driven with f_4 to transfer $|A_m^{(-)}, 0\rangle \rightarrow |g_m, 0\rangle$, while $f_1 - \nu$ and $f_4 - \nu$ are applied to ion n to drive sidebands $|e_n, 1\rangle \rightarrow |A_n^{(+)}, 0\rangle$ and $|g_n, 1\rangle \rightarrow |A_n^{(-)}, 0\rangle$. After this transfer, assuming it is imperfectly executed due to a pulse area error shared by all three tones, the system is in the state

$$|\phi_2\rangle = \cos\left(\frac{\delta\pi_2}{2}\right)|\psi_2\rangle - \sin\left(\frac{\delta\pi_2}{2}\right)|\psi_1\rangle, \quad (11)$$

where

$$|\psi_2\rangle \equiv -(c_{gg}|g_m, g_n\rangle + c_{ge}|g_m, e_n\rangle + c_{eg}|A_m^{(+)}, A_n^{(-)}\rangle + c_{ee}|A_m^{(+)}, A_n^{(+)}\rangle) \otimes |0\rangle, \quad (12)$$

and which is in form (7) with $\epsilon = -\sin(\delta\pi_2/2)$.

At this point, the residual populations that need to be optically pumped to the ground state ($|A_m^{(-)}, 0\rangle$, $|g_n, 1\rangle$, and $|e_n, 1\rangle$) are close in energy to populated levels. If the resolution of

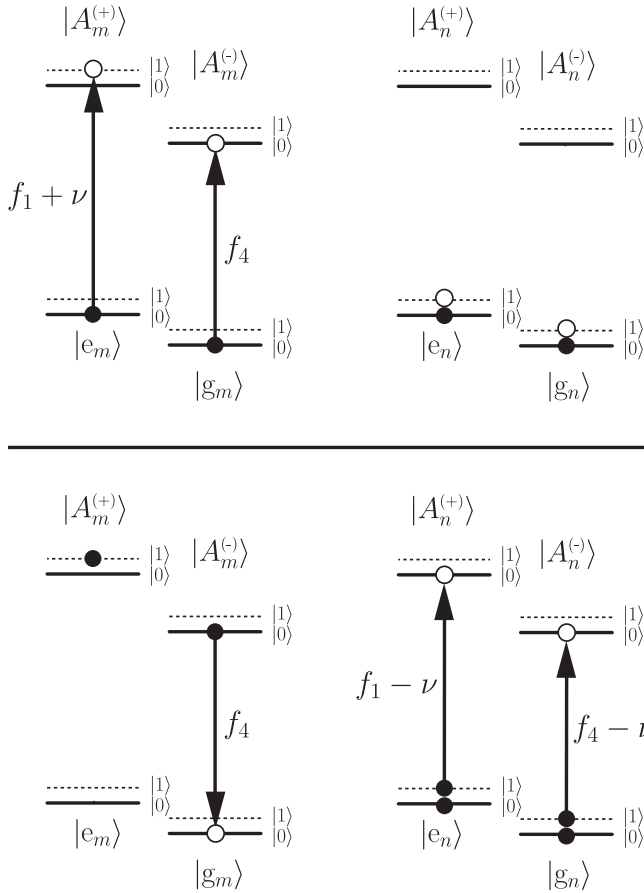


FIG. 2. Protocol for a certified Cirac-Zoller entangling gate between ion m (left) and ion n (right). The top panel shows the first transfer, which would be followed by optical pumping of any remaining population in the qubit manifold of ion m . The second transfer is shown in the bottom panel, which would also be followed by state-selective optical pumping of leftover population to the ${}^2S_{1/2}$ state. Transfer three is the reverse of the lower panel (with a phase shift of π added to $f_1 - \nu$), and transfer four is the reverse of the upper panel.

the optical pumping step is sufficient for this, they can be cleaned out directly; if not, a multistep transfer-then-pump process involving additional resolvable auxiliary states may be required. In either case, once this step has been completed

(and assuming neither ion is in the bright state), the system is left in $|\psi_2\rangle$.

The next step is almost identical to the preceding one: f_4 is applied to ion m and $f_1 - \nu$ and $f_4 - \nu$ are applied to ion n . However, a phase shift of π is added to tone $f_1 - \nu$ (which is on ion n only) for this transfer. Once the transfer attempt is completed, clean out of the auxiliary manifold of ion n and the $|g_m\rangle$ level of ion m will leave the system in

$$|\psi_3\rangle = i c_{gg} |A_m^{(-)}, g_n, 0\rangle + i c_{ge} |A_m^{(-)}, e_n, 0\rangle + i c_{eg} |A_m^{(+)}, g_n, 1\rangle - i c_{ee} |A_m^{(+)}, e_n, 1\rangle. \quad (13)$$

The last step is the same as the first, but with the subsequent clean out occurring on the auxiliary manifold of ion m . Again conditioned on the fact that the ions are not in the bright state, the motion factors and the final state of the two-ion system is

$$|\psi_4\rangle = U_{CZ} |\psi_0\rangle = (c_{gg} |g_m, g_n\rangle + c_{ge} |g_m, e_n\rangle + c_{eg} |e_m, g_n\rangle - c_{ee} |e_m, e_n\rangle) \otimes |0\rangle. \quad (14)$$

The state in Eq. (14) is identical to the result of an ideally executed the CZ gate, which can perform a CNOT gate with the addition of some single-qubit rotations [11]. However, each step can now be checked for errors that affect the pulse area of the simultaneous tones the same way, such as a drift in signal strength. Upon passing the check, subsequent gates will not be susceptible to correlated error accumulation from the errors removed by this scheme.

We have introduced here methods that allow certification of all of the gates required for universal quantum computation against common-mode pulse area errors. However, the classes of errors that are encountered in implementations of quantum processors go well beyond the limited class addressed here, as do the details for how these systems are made to execute their universal set of gates. The general approach we have sketched for developing certification should be adaptable to some of these situations, and extensions of these ideas may be possible moving forward.

W.C.C. acknowledges helpful discussions with Dave Hayes, Eric Hudson, Paul Hamilton, David Hucul, and David Allcock. This work was supported by the U.S. Army Research Office under Grant No. W911NF-19-S-0011 and the U.S. National Science Foundation under Awards No. PHY-1912555 and No. 2016245.

- [1] J. Preskill, *Quantum* **2**, 79 (2018).
- [2] F. Arute *et al.*, *Nature (London)* **574**, 505 (2019).
- [3] P. W. Shor, *SIAM J. Comput.* **26**, 14841509 (1997).
- [4] J. A. Sherman, M. J. Curtis, D. J. Szwer, D. T. C. Allcock, G. Imreh, D. M. Lucas, and A. M. Steane, *Phys. Rev. Lett.* **111**, 180501 (2013).
- [5] L. M. K. Vandersypen and I. L. Chuang, *Rev. Mod. Phys.* **76**, 1037 (2005).
- [6] R. Blume-Kohout, J. K. Gamble, E. Nielsen, K. Rudinger, J. Mizrahi, K. Fortier, and P. Maunz, *Nat. Commun.* **8**, 14485 (2017).
- [7] K. R. Brown, A. C. Wilson, Y. Colombe, C. Ospelkaus, A. M. Meier, E. Knill, D. Leibfried, and D. J. Wineland, *Phys. Rev. A* **84**, 030303(R) (2011).
- [8] J. E. Christensen, D. Hucul, W. C. Campbell, and E. R. Hudson, *npj Quantum Inf.* **6**, 35 (2020).
- [9] P. Taylor, M. Roberts, G. M. Macfarlane, G. P. Barwood, W. R. C. Rowley, and P. Gill, *Phys. Rev. A* **60**, 2829 (1999).
- [10] Conrad Roman *et al.* (personal communication).
- [11] J. I. Cirac and P. Zoller, *Phys. Rev. Lett.* **74**, 4091 (1995).